Bull. Korean Math. Soc. **41** (2004), No. 2, pp. 283–297

ON THE STRUCTURE OF A MUSH

YOUNG-KYUN YANG AND JOUNG-NAM LEE

ABSTRACT. We have obtained a simplified model for the mush under the assumption of the temperature, the solid fraction and the vertical component of the velocity, depend on upward coordinate z only. We have found solutions in the asymptotical limit and solved numerically for the model.

1. Introduction

During solidification of a liquid of two or more components with sufficiently high solutal concentrations, the planar freezing surface is morphologically unstable (Mullins and Sekerka [11]) and solidification is dendritic. As a result, the melt is separated from the eutectic solid by a region consisting of solid dendrites and interdendritic liquid, generally referred to as the mushy zone.

It is observed in experiments involving the solification of an ammonium chloride solution (Roberts and Loper ([10]), Chen and Chen ([2]) and Tait and Jaupart ([13])) that finger-like convection starts in the fluid region just above the mush soon after the experiments are initiated, and it coexists for a while with plume convection with associated chimneys in the mush. As the plume convection becomes stronger with time, the fingers weaken and eventually completely disappeared, so that the upward convection is carried entirely by the plumes. We observe something resembling a steady state in which the mush-liquid interface defined by the tops of the dendrite trees rises with a constant speed. We analyze this last stage of the experiments in which the chimneys and flow are fully developed.

Received May 20, 2003.
2000 Mathematics Subject Classification: 74N20, 76R10, 76S05, 80A22.
Key words and phrases: convection, phase change.
This paper was supported by the research fund of Seoul National University of Technology.

We seek solutions independent of time t in a frame fixed to the mush-solid interface, which moves upward relative to the solid with a prescribed constant speed U. The liquid region has fixed temperature T_∞ and composition ξ_∞ of light constitutent as $z \to \infty$, where z measures vertical displacement in the moving frame. The temperature decreases downward, and we consider the case in which a mushy zone separates a completely solid region from a completely liquid region. In this model problem we assume that the eutectic front, at which the temperature is equal to the eutectic temperature T_e and below which the system is completely solid, can be maintained at (or very close to) the fixed position $z = 0$. The mush-liquid interface $z = h$ is a free boundary to be determined as part of the solution. In general $h = h(x, y)$ though, in our case, it will be assumed a constant, as suggested by the experiments of ammonium chloride solution (Roberts and Loper ([10]), Chen and Chen ([2])).

We introduce a set of governing equations and boundary conditions for a mush that have been proposed by Hills, Loper and Roberts ([8]), based on principles of diffusive mixture theory. First, we treat the mush as a new single continuum phase. The temperature and the composition of solute in the interstitial fluid are approximately uniform on the scale that is small compared with the macroscopic dimensions of the system but large compared with the pore size between the crystals of the matrix. Second, we assume that the mush is in a complete local equilibrium at all times. In other words, the time-scales of melting and freezing processes are negligibly short compared with those of principal interest in studying the evolution of the mushy zone. A system in motion is clearly not in thermodynamic equilibrium, but if the motion is sufficiently slow a state close to local thermodynamic equilibrium will prevail. Thus, although the representative points in the phase plane for elements of solid and liquid phase will not lie precisely on solidus and liquidus, we are entitled, when the system evolves sufficiently slowly, to consider that they do so.

We let ξ^m, ξ^l and ξ^s be the mass fraction of light constitutent of the mixture, liquidus, and solidus, respectively, and let ϕ be the mass fraction of solid. Then ξ^m and ϕ are related by the so called 'lever rule',

$$\xi^m = \phi\xi^s + (1 - \phi)\xi^l. \tag{1.1}$$

With ξ^m being directly externally prescribed and ξ^l and ξ^s being indirectly prescribed through T, (1.1) solves for ϕ.

Note that for convenience, we will use the simple notation ξ for ξ^l from now on.

The density is defined as

$$\rho = \rho^s + \rho^l, \tag{1.2}$$

where

$$\rho^s = \phi\rho, \qquad \rho^l = \rho(1-\phi), \tag{1.3}$$

are respectively mass of solid and liquid per unit volume of mixture ; these partial densities are related to the actual solid and liquid densities ρ_s and ρ_l by

$$\rho^l = \rho_l\chi, \qquad \rho^s = (1-\chi)\rho_s, \tag{1.4}$$

where χ is the liquid volume fraction.

The barycentric velocity $\mathbf{u}$ is defined as

$$\rho\mathbf{u} = \rho^s\mathbf{u}^s + \rho^l\mathbf{u}^l. \tag{1.5}$$

If we substitute (1.3) into (1.5), the barycentric velocity may be expressed as

$$\mathbf{u} = \mathbf{u}^s + \mathbf{w}, \tag{1.6}$$

where

$$\mathbf{w} = (1-\phi)(\mathbf{u}^l - \mathbf{u}^s), \tag{1.7}$$

is the mass flux of interdendritic fluid relative to the solid phase. In this study, the density is treated as a constant everywhere except in the buoyancy term and the solid phase is constrained to move in rigid-body motion. Now conservation of total mass requires that

$$\nabla\cdot\mathbf{w} = 0. \tag{1.8}$$

We assume that the thermal conductivity, the specific heat per unit volume and the latent heat of solidification per unit volume, are constant and independent of phases. Also, we assume that the solutal diffusivity in the liquid is constant and the diffusivity in the solid phase is neglected.

The equations describing conservation of a constitutent in the liquid phase and energy in both phases can be written as

$$\frac{D_s\xi}{Dt} + \mathbf{w}\cdot\nabla\xi = \frac{D_s(\phi\xi)}{Dt} + D_o\nabla\cdot((1-\phi)\nabla\xi), \tag{1.9}$$

$$\rho_r c_p\left(\frac{D_sT}{Dt} + \mathbf{w}\cdot\nabla T\right) = k\nabla^2T + \rho_r L\frac{D_s\phi}{Dt}, \tag{1.10}$$

where D_o is the material diffusivity in the liquid phase, L is the latent heat, c_p is the specific heat, k is the thermal conductivity, ρ_r is a reference density, and $D_s/Dt = \partial/\partial t + \mathbf{u}^s\cdot\nabla$ is the material derivative

following the solid phase. The first term on the right hand side of the equation (1.9) represents the increase (or decrease) of composition of the liquid due to freezing (or melting) of the solid phase, while the second is the Fickian diffusive term which is commonly negligibly small. The first term on the right hand side of the equation (1.10), represents the thermal diffusion, and the second is the release (absorption) of latent heat of fusion as solid phase freezes (melts).

The solid phase is assumed to be rigidly attached to a substrate so that only the motion of the liquid phase is of concern. The percolation of the liquid phase relative to the solid is assumed to be governed by Darcy's law:

$$\frac{\eta \mathbf{w}}{\gamma(1-\phi)^2} = -\nabla p - (\rho^l - \rho_r) g \mathbf{z}, \tag{1.11}$$

where η is the dynamic viscosity of the liquid, p is the dynamic pressure *i.e.* with the hydrostatic pressure field subtracted, g is the gravity, $\mathbf{z}$ is the unit upward vector, and γ is the permeability of the mush.

The permeability γ is a function of both the mush porosity $\chi = 1 - \phi$ and the morphology of the crystal interfaces within it. Many different empirical and semi-empirical relationships for γ have been determined for various porous media. One example is the Kozeny equation which gives $\gamma = c_o \chi^3 / M^2$, where c_o is a constant and M is the specific surface area of the phase boundaries per unit volume of the porous media. This illustrates the general trends of all such formulae, namely that γ increases with the porosity and decreases with the specific surface area. Worster ([15]) used

$$\gamma = \gamma_o \chi^3, \tag{1.12}$$

which is suggested by the form of the Kozeny equation with M held constant. We note that the Kozeny-Carmen equation $\gamma = \chi^3 d^2 / 180(1-\chi)^2$ (d is the base diameter of a slender cone approximating the dendrite.) used by Chen and Chen ([2]), in which $\gamma \to \infty$ as $\chi \to 1$, is inappropriate when, as in this study, the Darcy equation is used to describe the flow in the porous medium rather than the more general Brinkman equation (Worster, [15]). We use equation (1.12) for the permeability. Since both thermal and compositional gradients exist across the mush, we must take account of both in calculating the overall density difference driving compositional convection. Thus, to determine the buoyancy forcing in (1.11), we use a linearized equation of state

$$\rho^l = \rho_r [1 - \alpha(T - T_r) - \beta(\xi - \xi_r)], \tag{1.13}$$

where α and β, are coefficients of thermal and compositional expansion, assumed constant, and T_r, ξ_r are reference values of the temperature and composition of the liquid. Note that β is positive since ξ is the mass fraction of light constitutent. Within the mush, this relationship can be written as

$$\rho^l = \rho_r[1 + (\frac{\beta}{\Gamma} - \alpha)(T - T_r)], \tag{1.14}$$

by taking the liquidus relationship

$$T = T_r - \Gamma(\xi - \xi_r) \tag{1.15}$$

into account, where the liquidus slope Γ is a positive constant. Note that $(\beta/\Gamma) - \alpha$ is usually positive since $\beta/(\alpha\Gamma)$ is typically much larger than unity. Now, if we substitute equation (1.14) into (1.11), we get

$$\frac{\eta \mathbf{w}}{\gamma(1-\phi)^2} = -\nabla p - \rho_r(\frac{\beta}{\Gamma} - \alpha)(T - T_r)g\mathbf{z}. \tag{1.16}$$

Equations (1.8), (1.9), (1.10), (1.15), and (1.16) constitute a full set of governing equations for the variables T, p, ξ, ϕ and $\mathbf{w}$ within the mush. Three interfacial conditions that express conservation of mass, energy and solute at both solid-mush and mush-liquid interfaces can be derived directly by integrating equations (1.8), (1.9) and (1.10) over an elementary volume enclosing (and collaping onto) each interface. These can be expressed as

$$[\mathbf{w} \cdot \mathbf{n}]_-^+ = 0, \tag{1.17}$$

$$\rho_r[-c_pT + L\phi]_-^+ V_n = [(-\rho c_p T(\mathbf{u}^s + \mathbf{w}) + \rho_r L\phi \mathbf{u}^s + k\nabla T) \cdot \mathbf{n}]_-^+, \tag{1.18}$$

$$[(1-\phi)\xi]_-^+ V_n = [((1-\phi)\xi \mathbf{u}^l - D_o(1-\phi)\nabla\xi) \cdot \mathbf{n}]_-^+, \tag{1.19}$$

where V_n is the normal velocity of the solid-mush or mush-liquid interface, $\mathbf{n}$ is a unit vector normal to the interface and the square brackets denote the jump in the enclosed quantity across the interface. Also, we require that the pressure, temperature and liquid composition be continuous at the mush-liquid interface, *i.e.*,

$$[p]_-^+ = 0, \qquad [T]_-^+ = 0, \qquad [\xi]_-^+ = 0. \tag{1.20}$$

Finally, we adopt a configuration of marginal thermodynamic equilibrium suggested by Worster ([14]), which is achieved if the temperature gradient on the liquid side of the mush-liquid interface is equal to the gradient of the local liquidus temperature. This is expressed by

$$\mathbf{n} \cdot \nabla T = -\Gamma \mathbf{n} \cdot \nabla \xi. \tag{1.21}$$

But, since we assume that the thermal conductivity is independent of phases, the marginal equilibrium condition (1.21) is equivalent to

$$\phi = 0, \tag{1.22}$$

on the mush-liquid interface (Worster, [14]).

Now, the boundary conditions to be applied to the mush-liquid interface are (1.17) through (1.20) and (1.22). The boundary conditions on the solid-liquid interface, consists of (1.17), (1.18), the second of (1.20) and

$$T = T_e, \tag{1.23}$$

where T_e denotes the eutectic temperature. Note that if growth is not eutectic, then the equation the second of (1.20) will be used instead of (1.23). (Fowler [6]).

We nondimensionalize the governing equations and boundary conditions by choosing a thermal length scale κ/U and thermal time scale κ/U^2, where κ is the thermal diffusivity $\kappa = k/\rho_r c_p$. Specifically, put $\mathbf{x} = (\kappa/U)\mathbf{x}^*$, $\mathbf{w} = U\mathbf{w}^*$, $p = \kappa\eta/\gamma_o p^*$, $\gamma = \gamma_o\gamma^*$, $T - T_r = (T_r - T_e)T^*$, $\xi - \xi_\infty = (\xi_e - \xi_\infty)\xi^*$, where T_r is the liquidus temperature of ξ_∞. Dropping the asterisks, (1.8)$\sim$(1.10), (1.15) and (1.16) become

$$\nabla \cdot \mathbf{w} = 0, \tag{1.24}$$

$$\mathbf{w}.\nabla\xi = \frac{\partial \xi}{\partial z} - \frac{\partial(\phi\xi)}{\partial z} - C\frac{\partial \phi}{\partial z}, \tag{1.25}$$

$$\mathbf{w} \cdot \nabla T = \nabla^2 T + \frac{\partial T}{\partial z} - S\frac{\partial \phi}{\partial z}, \tag{1.26}$$

$$T = -\xi, \tag{1.27}$$

$$\frac{\mathbf{w}}{\gamma(\phi)(1-\phi)^2} + \nabla p + R_a T\mathbf{z} = 0. \tag{1.28}$$

The parameters are a Stefan number $S = L/c_p(T_r - T_e)$, which represents the ratio of the latent heat needed to melt the solid and the heat needed to warm the solid from its eutectic temperature to the reference temperature T_r, the ratio of composition $C = \xi_\infty/(\xi_e - \xi_\infty)$, which denotes the compositional contrast between solid and liquid phases compared to the typical variations of concentration within the liquid (Worster ([15])), and a Rayleigh number $R_a = \gamma_o\rho_r(\beta - \alpha\Gamma)g(T_r - T_e)/V\eta\Gamma$, which will act to drive buoyancy induced convection in the mush if it is large enough. Note that very large Lewis number $Le = \kappa/D_o$ is assumed in equation (1.26). Boundary conditions are:

(i) on the liquid-mush interface, $z = h$

$$\phi = 0, \qquad [\mathbf{w} \cdot \mathbf{z}]^+_- = 0, \qquad [p]^+_- = 0, \qquad [\xi]^+_- = 0,$$

$$[T]^+_- = 0, \qquad [\frac{\partial T}{\partial z}]^+_- = 0, \qquad [\frac{\partial \xi}{\partial z}]^+_- = 0.$$

(ii) on the solid-mush interface, $z = 0$

$$\mathbf{w} \cdot \mathbf{z} = 0, \qquad T = -1, \qquad \xi = 1.$$

2. Asymptotical solutions

In this section, we first determine boundary conditions on the mush at the mush-liquid interface by using solutions in the liquid region which are obtained from assuming that the liquid region overlying the mush has uniform vertical motion. Then we assume in the mush that T, ϕ and w depend on height z only and the thickness of the mush is constant. We develop a simple set of equations for T, ϕ and w. Finally, we present asymptotical solutions of the model in case of $w << 1$.

We assume that the liquid region overlying the mush has uniform vertical motion. Then we obtain from equations (1.9) and (1.10)

$$T = T^*_\infty + (T_h - T^*_\infty)e^{-(z-h_0)(1+w_h)}, \tag{2.1}$$

and

$$\xi = \xi_h e^{-Le(z-h_0)(1+w_h)}, \tag{2.2}$$

where h_0 is the constant thickness of the mush,

$$T_h = T(h_0), \qquad \xi_h = \xi(h_0) \qquad w_h = w(h_0) \qquad T^*_\infty = \frac{T_\infty - T_r}{T_r - T_e}.$$

If we apply to (2.1) and (2.2) the marginal equilibrium condition in the liquid $(\frac{\partial T}{\partial z})_l = -(\frac{\partial \xi}{\partial z})_l$, the liquidus relation $T_h = -\xi_h$, and $[T]^+_- = 0$ at $z = h_0$, we obtain, to dominant order in powers of Le^{-1},

$$T_h = 0, \quad \xi_h = 0. \tag{2.3}$$

We use (2.3) as boundary conditions when we find solutions of the mush.

We assume that the temperature T, the mass fraction of the solid ϕ and the vertical component of the velocity $-w$ depend on z only. Then we obtain from equations (1.24) $\sim$ (1.27) the set of governing equations and boundary conditions for a mush as follows.

$$T' = (C + S - T)\phi + H, \tag{2.4}$$

where $H = T'(h_0)$ measures the amount of superheat.

$$\phi' = \frac{T'}{T - C}(1 + w - \phi). \tag{2.5}$$

$$w' = V(1 - \phi)^5, \tag{2.6}$$

where $V = w'(h_0)$. Note that we use the permeability relation $\gamma(\phi) = (1 - \phi)^3$ from Worster ([15]). The boundary conditions are

$$T(h_0) = 0, \qquad \phi(h_0) = 0, \qquad T(0) = -1, \qquad w(0) = 0. \tag{2.7}$$

Note that we use the third condition in (2.7) to find the thickness h_0 of the mush.

We assume that $w << 1$. Then from (2.5), we have

$$\phi' = \frac{T'}{T - C}(1 - \phi). \tag{2.8}$$

From (2.8) we obtain

$$\phi = \frac{T}{T - C}, \tag{2.9}$$

where the conditions $T_h = 0$ and $\phi_h = 0$ were used. The solution (2.9) for ϕ reveals that the solid fraction in the mush decreases when the temperature increases, and shows that the ratio of composition C affects the distribution of solid in the mush.

Let's discuss physics of the expression of (2.9). Since $T = -\xi$, we rewrite (2.9) as

$$C\phi - (1 - \phi)\xi = 0. \tag{2.10}$$

On the other hand, since we assume $\xi^s = 0$, the scaled mass fraction ξ^m of light constitutent of the mush is from (1.1)

$$\xi^m = -C\phi + (1 - \phi)\xi. \tag{2.11}$$

From (2.10) and (2.11), we have

$$\xi^m = 0. \tag{2.12}$$

Note that the scaled mass fraction of light component of the liquid is zero from (2.2) and the second of (2.3). Therefore, (2.12) means that the mass fraction of light component of the liquid and the mush are equal. This denotes the fact that the mass of light constitutent of the liquid is conserved through the mush when convection is absent.

We next find an implicit expression for the temperature. If we substitute (2.9) into (2.4), we get

(2.13)

$$z = \frac{1}{2}\ln\frac{1+a+b}{T^2-aT+b} + \left(\frac{2C-a}{2\sqrt{d}}\right)\ln\frac{a+2b+\sqrt{d}-T(2+a-\sqrt{d})}{a+2b-\sqrt{d}-T(2+a+\sqrt{d})},$$

where $a = C + S + H$, $b = CH$, $d = a^2 - 4b$. The depth of the mush is obtained by setting $z = h_0$, $T = 0$ in (2.13).

We present figure 2 to show how the solid fraction and the temperature can vary with height. We see that C affects the distribution of solid in the mush and thus the mobility of the interstitial fluid and the nature of any flow that might take place.

When C is large or moderate, the solid fraction is small throughout the mush. (see the solid and dashed curves in figure 2). This suggests that the permeability is large and its change is small with depth. This situation, in particular, shown in the solid line of figure 2, is typical of the ammonium-chloride experiments. When C is small, ϕ is large relatively through much of the mush. This indicates that the permeability is small, it is likely to be a strong function of depth and fluid flow may only penetrate the upper portions of the mush. This case corresponds to the Pb-10 wt%Sn experiment (Hellawell *et al.*, [7]). (see the dotted curves in figure 2).

We consider some asymptotic cases of (2.13), in order to understand how the system depends on the three dimensionless parameters C, S and H.

If $C >> 1$ or $S << 1$, then

$$z = \ln\frac{H+1}{H-T}, \tag{2.14}$$

so that

$$h_0 = \ln(1+\frac{1}{H}). \tag{2.15}$$

We see that the depth h_0 of the mush dominantly depends upon thermal balances between conduction of heat through the mush and conduction of heat from the liquid region in determining h_0.

We let $\Omega = S$ or H. If $\Omega >> 1$, then

$$z = \ln\frac{\Omega+1}{\Omega-T}. \tag{2.16}$$

In this case,

$$h_0 \to 0, \tag{2.17}$$

the thickness of the mush is small due to the dominant influence of conduction of heat from the liquid region or the dominant influence of the latent heat released during solidification.

If $C << 1$, then

$$z = \ln \frac{H+S+1}{H+S-T}, \tag{2.18}$$

therefore,

$$h_0 = \ln(1 + \frac{1}{H+S}). \tag{2.19}$$

In this case, h_0 is determined by balancing conduction of heat through the mush, conduction of heat from the liquid region, and the latent heat released during solidification.

Lastly, we consider in case that heat transfer from the liquid region is weak. We let $H << 1$. Then we have

$$h_0 \sim \frac{C}{C+S} \ln \frac{C+S}{CH}, \tag{2.20}$$

which indicates the effects of C in determining h_0. We see that increasing C is equivalent to decreasing S and thus that varying C acts to modify the amount of latent heat released.

3. Numerical solutions for a mush

In this section, we solve numerically the set of equations (2.4), (2.5) and (2.6). Then we compare them with asymptotical solutions.

It is not easy that the numerical integration of the set of equations (2.4), (2.5) and (2.6) satisfies two bottom boundary conditions at the same time when we integrate from the top of the mush $z = h_0$. We therefore integrate first the following equations (3.1), (3.2) from $T = 0$ to $T = -1$, which can be obtained from (2.4), (2.5) and (2.6).

$$\frac{d\phi}{dT} = \frac{1+w-\phi}{T-C} \tag{3.1}$$

$$\frac{dw}{dT} = \frac{V(1-\phi)^5}{(C+S-T)\phi + H} \tag{3.2}$$

with conditions

$$\phi(0) = 0, \qquad w(-1) = 0. \tag{3.3}$$

In our system, we have five parameters, *i.e*, $w_h = w(h_0)$, $V = w'(h_0)$, S, C, $H = T'(h_0)$. Both C and S are experimentally controllable parameters. Since it can be shown that H depends on w_h, we actually have two internal parameters. Given w_h, the value of V is determined numerically by stopping condition $w(-1) = 0$.

Then we next integrate equations (2.4), (2.5) and (2.6) numerically with the values of parameter obtained from the above numerical solutions. We obtain valid numerical solutions of T, ϕ, and w if the third and the fourth condition in (2.7) are satisfied at the same time. (see the solid curves in figures 3 and 4).

As we see from figure 3 and 4, our numerical solutions (the solid curves) consistent with the asymptotical solutions (the dashed curves) in the qualitative sense. When C is large, the solid fraction ϕ is small throughout the mush as we see from figure 3 corresponding to the ammonium chloride experiments. This means, in case of the ammonium chloride experiments, that the permeability is relatively large and the variation of the permeability is small with depth. When C is small, from figure 4 corresponding to the Pb-10wt%Sn experiments, we see that ϕ is comparatively large except the upper portions of the mush. This indicates, for the metallic lead-tin alloy, that the permeability is likely to be a strong function of depth and fluid flow hardly penetrates the bottom parts of the mush.

4. Experiment and comments

The laboratory experiment is easy to perform and makes a simple and attractive fluid-dynamical demonstration. A warm aqueous ammonium chloride solution (for example, 28wt%NH_4Cl) of composition more concentrated than the eutectic value (20wt%) is placed in a suitable container (a glass beaker will do) and cooled from below, for example by placing the glass beaker on a bed of ice. After a short while the bottom of the beaker is completely covered with small dendritic crystals of ammonium chloride and the thickness of the layer gradually increases with time. It appears that a planar solid-liquid interface is highly (morphologically) unstable, and that the actual interface is a highly irregular surface, which takes the form of small dendrite arms occupying a zone of finite thickness, often called the mushy zone. The reason for this fact is that a planar interface leads to 'constitutional' supercooling, where the liquid ahead of the interface has a temperature below the liquidus,

despite being above the interfacial temperature, because of the dependence of the liquidus (freezing) temperature on solute concentration. The common occurrence of dendritic or mushy zones is due to the fact that compositional diffusivities are invariably much smaller than thermal diffusivities, so that the thickness of the region over which the concentration changes in the liquid is much thinner than the corresponding region over which the temperature changes.

In the early stages, finger-like convection starts in the fluid region just above the mush. With increased time, plumes with associated chimneys are visible. During an extended period these coexist with the fingers. The finger convection become progressively weaker and chimneys are eventually the only sites of upwelling. Downward flow in the mush causes solidification and upward flow promotes dissolution. The nonlinear interaction of dissolution and convection leads to the formation of chimneys.

The NH_4Cl solution above the mush remains continually undersaturated. The circulation above the mush consists of upward flow in isolated buoyant plumes which is compensated by a downward return flow of the undersaturated solution. This liquid slowly migrates towards the layer of crystals and flows down to it. Because the flow through the crystals takes place in a decreasing temperature field, the aqueous solution becomes saturated and NH_4Cl exsolves onto existing NH_4Cl crystals, which exhibit secondary and tertiary branching. The NH_4Cl-depleted solution from a wide area within the mush flows to a central point and the less-dense return flow takes place through a few isolated chimneys. The upward flow in the plume induces motion of the bulk fluid toward the plume itself. The comparatively solute-rich fluid, meeting the cold plume, tends to crystallize around the chimney. As a result, there is a buildup of crystals around each chimney exit, like a mini-volcano. With time some chimneys become inactive and the overall intensity of the convective motion decreases as the thickness of the mushy layer increases.

As we see from experiment, a mush-chimney system has three components: the main body of mush where downward vertical flow is dominant, the chimney wall where the fluid flows into the chimney horizontally, and the chimney where the fluid flows upward.

In this paper, we have found solutions in the asymptotical limit and solved numerically for the main body of mush. The remaining work is to analyze the chimney wall and the chimney by using our model. In the distant future, we will work try to answer whether any of the family of solutions found from the governing equations for the of mush are stable

and whether, therefore, they correspond to experimentally observable states.

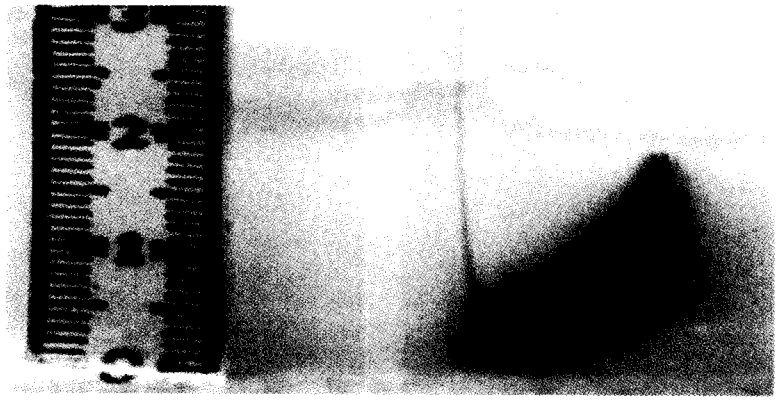

Figure 1.– a close-up picture of the mush-chimney system. We see that the mush generally consists of vertical or nearly vertical primary dendrites with secondary and tertiary arms. It shows that the NH_4Cl-depleted fluid is sucked into the chimney and rises up into the melt due to its own compositional buoyancy. It was taken from $28\%NH_4Cl$-H_2O solution experiment two hours after the experiment started.

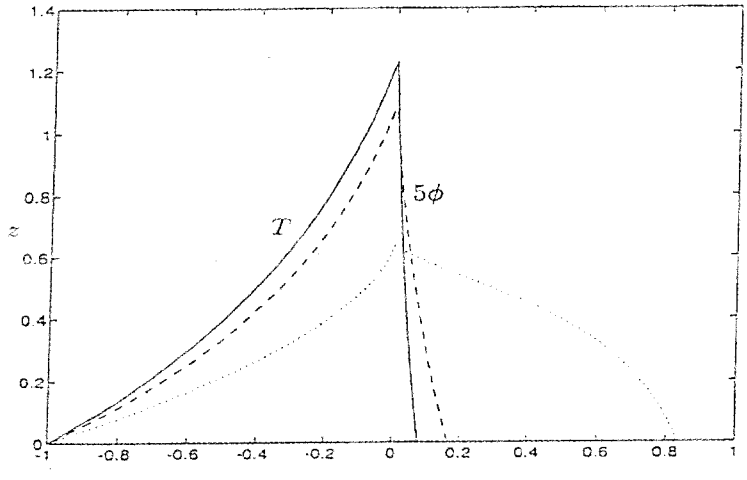

Figure 2.– The solid graphs show the temperature T and the solid fraction ϕ in case of $C = 74/6$. The dashed and dotted curves represent T, ϕ when $C = 5.0$ and $C = 0.2$ respectively.

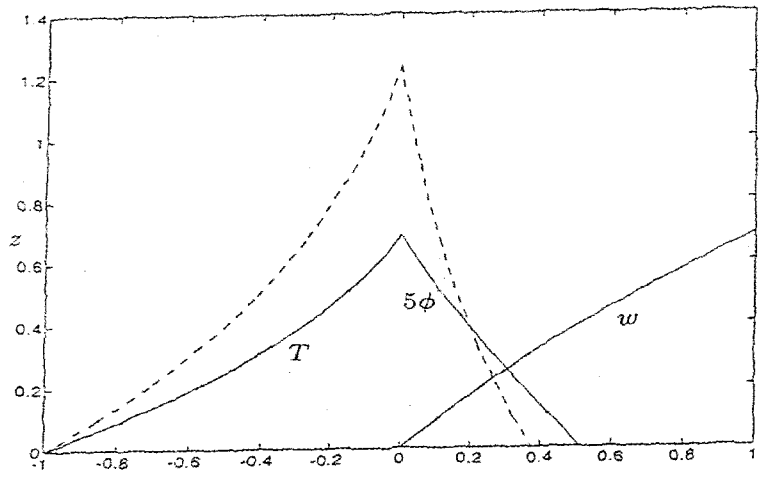

Figure 3.– The solid graphs present T, ϕ and w as functions of z when $C = 74/6$ and $w_h = 1.0$. The dashed curves are the solid graphs in figure 2.

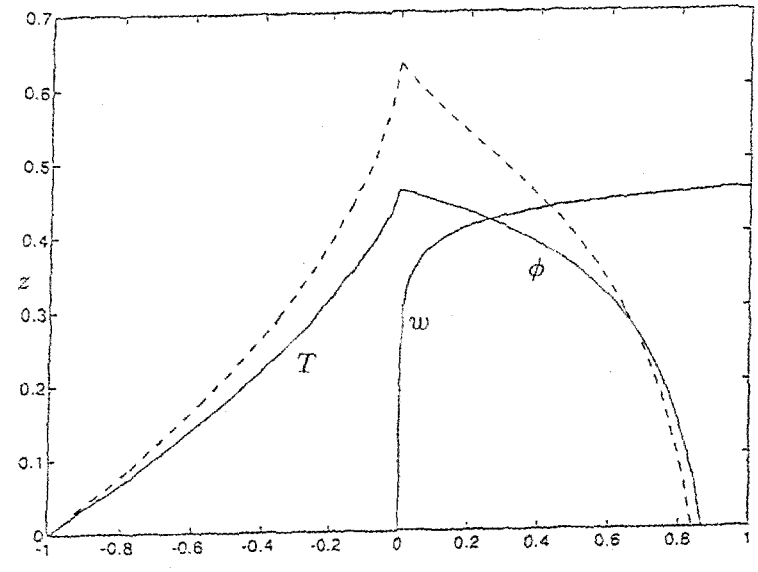

Figure 4.– The solid graphs present T, ϕ and w as functions of z when $C = 0.2$ and $w_h = 1.0$. The dashed curves are the dotted graphs in figure 2.

References

[1] B. Chalmers, *Principles of solidification*, Wiley, New York, 1964.

[2] C. F. Chen and F. Chen, *Experimental study of directional solidification of aqueous ammonium chloride solution*, J. Fluid Mech. **227** (1991), 567–586.

[3] C. A. Chung and M. G. Worster, *Steady-state chimneys in a mushy layer*, J. Fluid Mech. **297** (1995), 387–411.

[4] S. M. Copley, A. F. Giamei, S. M. Johnson, and M. F. Hornbecker, *The origin of freckles in unidirectionally solidified castings*, Metall. Trans. **1** (1970), 2193–2204.

[5] D. L. Feltham and M. G. Worster, *Flow-induced morphological instability of a mushy layer*, J. Fluid Mech. **297** (1999), 337–357.

[6] A. C. Fowler, *The formation of freckles in binary alloys*, IMA J. Appl. Math. **35** (1985), 159–174.

[7] A. Hellawell, J. R. Sarazin, and R. S. Steube, *Channel convection in partly solidified systems*, Phil. Trans. R. Soc. Lond. **A 345** (1993), 507–544.

[8] R. N. Hills, D. E. Loper, and P. H. Roberts, *A thermodynamically consistent model of a mushy zone*, Q. J. Mech. Appl. Math. **36** (1983), 505–539.

[9] H. E. Huppert and M. G. Worster, *Dynamic solidification of a binary alloy*, Nature **314** (1985), 703–707.

[10] P. H. Roberts and D. E. Loper, *Towards a theory of the structure and evolution of a dendrite layer*, In Stellar and Planetary Magnetism (Soward, A. M., Ed.) 1983, 329–349.

[11] W. W. Mullins and R. F. Sekerka, *Stability of a planar interface during solidification of a dilute binary alloy.*, J. Appl. Phys. **35** (1964), 444–451.

[12] T. P. Schulze and M. G. Worster, *A numerical investigation of steady convection in mushy layers during the directional solidification of binary alloys*, J. Fluid Mech. **356** (1998), 199–220.

[13] S. Tait and C. Jaupart, *Compositional convection in a reactive crystalline mush and the evolution of porosity*, J. Geophys. Res. **97** (B5) (1991), 6735–6756.

[14] M. G. Worster, *Solidification of an alloy from a cooled boundary*, J. Fluid Mech. **167** (1986), 481–501.

[15] ———, *Natural convection in a mushy layer*, J. Fluid Mech. **224** (1991), 335–359.

School of the Liberal Arts, Seoul National University of Technology, Seoul 139-743, Korea

E-mail: ykyang@snut.ac.kr
ljnam@snut.ac.kr